Marine Biology (2003) 143: 427–441
DOI 10.1007/s00227-003-1100-1

M. Maldonado · M. Durfort · D. A. McCarthy
C. M. Young

The cellular basis of photobehavior in the tufted parenchymella larva of demosponges

Received: 15 January 2003 / Accepted: 18 April 2003 / Published online: 29 May 2003

Abstract The mechanisms by which light elicits a phototactic response in sponge larvae remain poorly understood. Here we investigate histological and behavioral aspects of the photoresponse in parenchymella larvae of three demosponges. Two species are photonegative during their entire larval life, while the other, initially photopositive, becomes photonegative only after swimming in the laboratory for 4 h to 6 h. All larvae are bullet-shaped, with a uniformly ciliated surface, except at their posterior end, which is unciliated but surrounded by a distinctive ring of long cilia, the tuft. The short cilia beat metachronally, generating the thrust to move the larva forward with clockwise rotation. The long cilia of the tuft do not beat metachronally and are apparently more involved in maneuvering than in the generation of thrust. Transmission electron microscopy revealed in one species that the axoneme of the short cilia contains a distinctive "9×3 + 2" microtubule pattern at its base, but the presence of such an arrangement in cilia of the tuft remains uncorroborated. Nevertheless, the differences in beating characteristics between the monociliated cells of the tuft and those in the rest of the body correspond to other cytological differences. Cilia of the tuft have a type-I basal body, a large basal foot, and a branched rootlet, whereas the remaining cilia have a type-II basal body, a smaller and simpler basal foot, and an unbranched rootlet. Furthermore, the cells forming the tuft have a characteristic distal protrusion filled with pigments and mitochondria. Several of these traits suggest that the monociliated cells of the tuft are involved in the larval photoresponse both as sensors and effectors. Drastic changes in light intensity have no effect on the beating of the short cilia. In contrast, they cause a predictable and instantaneous movement of each cilium in the tuft, triggering expansions and contractions of either a part or the entire tuft, which in turn alters the direction of swimming. Observations on free-swimming larvae suggest that the tuft works as a passive light-sensitive rudder in both photonegative species that contract their posterior cilia under high irradiance and in photopositive species that expand their cilia under high irradiance. However, in photonegative larvae that expand the tuft under high irradiance, an active ciliary coordination by the larva needs to be invoked to explain a deviation of the swimming trajectory.

Communicated by S. A. Poulet, Roscoff

M. Maldonado (✉)
Department of Aquatic Ecology,
Centro Estudios Avanzados de Blanes (CSIC),
Acceso a Cala St. Francesc 14,
17300 Blanes, Girona, Spain
E-mail: maldonado@ceab.csic.es
Tel.: +34-972-336101
Fax: +34-972-337806

M. Durfort
Department of Cell Biology, Faculty of Biology,
Universidad de Barcelona, Avenida Diagonal 645,
08071 Barcelona, Spain

D. A. McCarthy
Department of Larval Ecology,
Harbor Branch Oceanographic Institution,
5600 U.S. Hwy 1 N.,
Fort Pierce, FL 34946, USA

C. M. Young
Oregon Institute of Marine Biology,
University of Oregon,
P.O. Box 5389, Charleston,
OR 97420, USA

Introduction

Nine larval types have been identified in Porifera so far (reviewed by Maldonado and Bergquist 2002). The parenchymella type is the larva of many demosponges, a group comprising the largest taxonomic class in the phylum Porifera. Parenchymellae are 150 to 5,000 μm in length, 30 to 500 μm in width, externally ciliated, solid, and have just a few cell types. They are lecithotrophic and dispersal time ranges from a few hours to several

days, depending on the species. Upon competency to settle, the free-swimming parenchymella becomes demersal, moving near the surface of potential settlement substrata. This presumed exploratory behavior lasts from a few hours to several days before attachment and metamorphosis of the larva into a juvenile sponge.

It is generally believed that sponge larvae competent for metamorphic induction are able to detect a variety of environmental stimuli (light, gravity, water movement, chemicals, etc), that either induce or inhibit their settlement (see reviews by Fry 1971; Sarà and Vacelet 1973; Fell 1974). This view contradicts the fact that sponge larvae are not known to have sensory organs for receiving stimuli or a nervous system for integrative signal processing. Such anatomical constraints should mean that sponge larvae have a limited ability for orientation and selection of suitable settlement sites, compared to those of other invertebrate larvae. Indeed, the available current literature on sponge larval ecology provides insufficient evidence to support the idea that sponge larvae can actively respond to such cues as gravity, prevailing currents, chemicals, or attached sponges. The arguments for such larval behavior are not supported by adequate experimental studies, and their validity remains questionable (Maldonado et al. 1997). However, this is not the case for larval photobehavior.

Many observations (e.g., Bergquist and Sinclair 1968; Sarà and Vacelet 1973; Fell 1974; Woollacott 1990, 1993) and experiments (e.g., Fry 1971; Maldonado and Young 1996; Maldonado et al. 1997; Maldonado and Uriz 1998; Leys and Degnan 2001; Uriz et al. 2001) document phototaxis in parenchymella of several sponge species during dispersal and settlement. Parenchymellae can perceive drastic changes in irradiance when swimming in and out of small pits and crevices, which presumably facilitates identification and subsequent settlement in shaded microhabitats. Sponge settlement in pits and crevices enhances juvenile survival (Maldonado and Uriz 1998), presumably by reducing exposure to silt, wave abrasion, predators, UV radiation and various other major mortality agents (Young and Chia 1984; Raimondi 1990; Bourget et al. 1994; Walters and Wethey 1996; Hills et al. 1998). Therefore, larval photoresponses appear to serve the same crucial adaptive role for many demosponges, as they do for other benthic invertebrates.

Interestingly, phototactic abilities vary with the ciliation pattern of the parenchymella. Parenchymella larvae may be: (1) entirely and uniformly covered by short cilia[1]; (2) entirely and uniformly covered by short cilia except for their posterior end, which is bare; or (3) entirely and uniformly covered by short cilia, except for their posterior end, which is bare but encircled by a distinctive ring of long cilia (tufted parenchymellae). Non-tufted parenchymellae are either moderately phototactic or photo-indifferent, while tufted larvae usually show intense phototactic responses (Kaye and Reiswig 1991; Woollacott 1990, 1993; Maldonado and Young 1996). Even some tufted larvae have the ability to modulate their photoresponse over time (Maldonado et al. 1997). Larvae of the haplosclerid sponge *Sigmadocia caerulea* remain intensely photonegative during their entire free-swimming life, yet newly released larvae swim away from an experimental light source at a significantly higher speed than late (30-h-old) larval stages. Furthermore, newly released larvae cease directional swimming after moving away only a short distance (15 cm on average) from the light source. In contrast, older larvae swim three times as far before stopping. At this distance, light intensity is about two orders of magnitude lower than that required for cessation of swimming by newly released larvae. Therefore, while the sign of phototaxis (direction of swimming with respect to the light source) remains consistent throughout larval development, both the photokinetic response (swimming velocity during response to light), and the minimum light threshold required to induce a larval response change with age.

The fact that parenchymellae can display such a relatively complex photobehavior is relevant not only from an ecological point of view, but also from an evolutionary perspective. The Porifera are regarded as simple, primitive metazoans that predate the evolutionary development of specialized eumetazoan systems for reception, conduction, and integration of external signals. Such an evolutionary status makes it hard to explain the photobehavior of tufted parenchymellae. Consequently, it cannot be ruled out that these larvae respond to light by very different mechanisms than those of higher metazoans. Indeed, very little is known about the cytological mechanisms responsible for larval sponge behavior. Pioneering TEM and SEM studies made notable contributions to the general cytology of the parenchymella (e.g., Lévi 1964; Boury-Esnault 1976; Evans 1977; Bergquist et al. 1979; Vacelet 1979). In the last decade, several excellent works have expanded our knowledge of the parenchymella cytology (e.g., Kaye and Reiswig 1991; Woollacott 1990, 1993; Amano and Hori 1994, 1996; Jaeckle 1995; Woollacott and Pinto 1995; Uriz et al. 2001). Despite these studies, the cytological basis of photobehavior remains poorly investigated, with only a one recent paper specifically addressing the topic (Leys and Degnan 2001). These authors presented evidence that the swimming trajectory of the photonegative parenchymella of a haplosclerid sponge can be mediated by autonomous, independent responses of individual cells in the ciliated posterior tuft of the larva. In this study, we investigated the cytology and behavior of tufted larvae of three demosponges

[1] The term "cilia" is hereafter used to refer to eukaryotic organelles that are structurally characterized by an essentially identical arrangement of microtubules. Following Nielsen (1987), this definition covers the undulating cilium of many protists and sperm cells to the planar cilium of vertebrate multiciliated cells. The term "flagellum" is used for simpler structures found in the bacteria, which lack microtubules.

from different taxa. Our research provides independent evidence to partially support the hypothesis advanced by Leys and Degnan (2001), but also proposes alternative mechanisms to explain how larvae effect deviation of their trajectory in response to light cues. We also present and discuss new information on potential correlations between larval phototaxis and ultrastructure.

Materials and methods

The current study is mostly based on cytological observations of *Sigmadocia caerulea* parenchymella (Porifera, Haplosclerida), the ecology and photobehavior of which were documented in previous studies (e.g., Maldonado and Young 1996, 1999; Maldonado et al. 1997). Complementary information on larval behavior and ciliary activity is provided by laboratory and field observations on the free-swimming parenchymella of *Ircinia oros* and *Cacospongia mollior* (Porifera, Dictyoceratida).

Collection of larvae

Brooding individuals of *S. caerulea* were obtained from a population living on rocks between 0.5 and 2 m deep in the Indian River Lagoon near Fort Pierce, Florida, USA during August 1996. Ripe sponges were induced to release larvae in the laboratory by being briefly exposed to air, following the methodology described in previous studies (Maldonado and Young 1996, 1999; Maldonado et al. 1997). Larvae of *I. oros* and *C. mollior* were obtained from a population found at 10–12 m depth off Blanes, Spain (western Mediterranean coast) during July and August 1999, 2000 and 2002. We collected larvae in situ using SCUBA and withdrawing larvae with a Pasteur pipette from the exhalant currents of sponges that were releasing larvae.

Observations on general swimming patterns and ciliary movement

Laboratory observations on different aspects of movement were made by viewing larvae in glass Petri dishes filled with 0.45-μm-filtered seawater collected from the habitats of the respective species (salinity of 34 for *S. caerulea* and 37 for *I. oros* and *C. mollior*) and maintained at room temperature (19–24°C). We also studied movement patterns in the field using SCUBA, monitoring free-swimming larvae ($n = 25$ per species) of *I. oros* and *C. mollior* at 10–12 m depth for approximately 10–30 min during late July 2000 and 2002. For some larvae ($n = 10$ per species), monitoring started immediately upon their release in the exhalant water flow of the parents. Whenever possible, divers remained motionless to avoid interfering with larval trajectories and natural patterns of larval swimming.

Observations on light-induced patterns of locomotion

We investigated light-induced patterns of locomotion in a laboratory dark room, using a 2-l, square aquarium made of UV-opaque methacrylate, in which larvae of *I. oros and C. mollior* were offered two light conditions (illuminated vs. shaded region). The illuminated region received 600 to 935 μ*M* photons m^{-2} s^{-1} via the beam of a cold light (Olympus Highlight 3100 illuminator) directed perpendicular to one of the aquarium sides and through a neutral diffuser. By covering half the lateral side of the aquarium with a black opaque plastic, we created a shaded region in which irradiance ranged from 1 to 40 μ*M* photons m^{-2} s^{-1}. Irradiance was measured by using both a LI-COR quantum meter provided with a LI-192SA underwater quantum sensor and a Li-189 photometer with a UWQ4783 sensor. To minimize distortion of the angular light distribution during the experiments compared to that occurring in the ocean, we placed the aquarium containing the larvae within a larger seawater aquarium, as suggested by Forward et al. (1984).

In these conditions, we recorded the positive (swimming within the illuminated region) or negative (swimming within the shaded region) sign of the larval phototaxis by monitoring the position of larvae ($n = 25$) in the aquaria after 15 min. To detect changes in the sign of phototaxis over time, we repeated the experiment at several larval ages (2 h, 4 h, 6 h, 8 h, 12 h, 24 h, and 48 h). We also investigated the role of the cilia of the larval tuft in effecting deviation of the swimming trajectory of 2-h and 8-h-old larvae ($n = 50$) as they entered the shaded portion of the aquarium from the illuminated part and vice versa. To this end, we monitored larvae through an Olympus SZX12 dissecting microscope provided with a SZ-STU2 support that allowed rapid horizontal displacements of the objective to follow moving animals in containers full of water.

To study movement of the larval cilia in further detail, larvae of all three species were placed in a small volume of seawater on excavated slides and observed through a Zeiss compound microscope for a few minutes. In these conditions, we examined the movement of larval cilia in response to different levels of irradiance (1 to 620 μ*M* photons m^{-2} s^{-1}). The level of irradiance was obtained by manipulating the aperture of the shutter and the emission intensity of the 6-W bulb of the microscope. Irradiance of larvae on the slides was measured by a Li-189 photometer with a UWQ4783 sensor in air mode. We also assessed the ciliary response to these light treatments by *I. oros* and *C. mollior* larvae ($n = 5$) after removal of the posterior end by a microscalpel, following the approach by Leys and Degnan (2001). Finally, whenever the experimental light conditions permitted, photographs of living larvae in the different experimental conditions were taken with both analogical and digital cameras connected to the dissecting and light microscopes.

Cytological study of larvae

ILarvae were fixed for transmission electron microscopy (TEM) in 2.5% glutaraldehyde in 0.2-*M* Millonig's phosphate buffer (pH 7.4) and 0.14-*M* NaCl for 1 h. They were then rinsed with phosphate buffer for 40 min, post-fixed in 2% OsO_4 in 0.2-*M* Millonig's phosphate buffer for 1 h, dehydrated in a graded series of ethanol, infused with propylene oxide, and then embedded in EPON 812 resin. Ultra-thin sections were stained with uranyl acetate and lead citrate, and examined in a Philips EM-301 electron microscope. Larvae were fixed for scanning electron microscopy (SEM) in a 6:1 (by volume) mixture of osmium tetroxide and saturated mercuric chloride solution in distilled water for 90 min. They were then dehydrated in an ethanol series, fractured in liquid nitrogen (if required), dried at the critical point, sputter-coated with gold, and examined in a Hitachi S-2300 electron microscope.

In describing the larval cytology, we will use the term "distal" to refer to the cell portion closer to the outer larval surface, and "proximal" for the opposite portion. We will use the term "anterior" to refer to the leading end of a swimming (not drifting) larva and "posterior" for the opposite end.

As part of the cytological study, we found that the free-swimming parenchymella may contain a total of 11 morphologically identifiable cell types, including 5 types exclusively located in the larval epithelium and 6 in the internal regions. The current investigation focuses only on 3 types of epithelial cells potentially involved in larval locomotion and photoresponse: 2 types of monociliated cells (one forming the tuft, the other providing the short ciliation of the remaining body) and the unciliated, flattened cells that form the epithelium of the posterior larval pole. The remaining cells, intercellular matrix structures, and symbiotic bacteria will be the subject of a separate study.

Results

General swimming patterns and ciliary movement

The parenchymellae of both species are prolate spheroids, with length and width measurements of (mean ± SD) 629 ± 95 × 275 ± 50 μm in *S. caerulea*, 690 ± 45 μm × 320 ± 15 μm in *I. oros*, and 700 ± 36 × 318 ± 26 μm in *C. mollior*. The larva of all three species have a densely and uniformly ciliated surface, except for a small portion of the anterior end and the whole posterior end, which is nearly flat and bare (Fig. 1A–H). The border between the posterior bare area and the lateral ciliated surfaces of the larva consists of a ring of brown-pigmented cells (Fig. 1A–E), from which a tuft of long cilia arises (Fig. 1A–I). The cilia of this posterior tuft are 140–160 μm in length in *I. oros* and *C. mollior* and 80–90 μm in *S. caerulea*. Cilia in the tuft are markedly longer than those at the remaining larval regions, which measure about 15–20 μm in length.

The tufted larvae of all three species are vigorous swimmers, able to effect rapid changes in their trajectory and swimming speed. The larvae of *S. caerulea, C. mollior,* and *I. oros* swim for an average of 2, 3 and 5 days, respectively, before settling in laboratory conditions. Larvae of *S. caerulea* and *I. oros* are negatively phototactic during their entire larval life, readily swimming away from artificial and natural light sources. However, all free-swimming larvae of *C. mollior* are initially photopositive in laboratory conditions, but then become photonegative after 4 h (56%) to 6 h (92%). As viewed from the posterior pole, larvae of all three species swim with the anterior pole directed forward while rotating clockwise around their longitudinal axis. The power for both forward motion and rotation is thought to be provided by the short cilia that cover the body. These cilia are organized in functional rows parallel to the larva's longitudinal axis, and beat with a planar effective stroke that is parallel to the longitudinal larval axis. The coordinated movement of these cilia generates waves that propagate from the anterior to the posterior larval end (i.e., diaplectic metachronism). They also travel across the longitudinal ciliary bands, moving to the right of the effective stroke (dexioplectic waves). Therefore, the thrust for forward motion is generated by the diaplectic metachronism, and the rotation results from the dexioplectic nature of the waves.

The posterior tuft is apparently more involved in maneuverability than in generation of thrust. Unlike the short cilia of the body, the long cilia of the posterior tuft look like macroscopically visible structures (Fig. 1A–H). However, further SEM and TEM observations corroborate that they are not substantially thicker than the remaining cilia of the body (see the cytology sections). Unlike the short cilia of the body, the long cilia of the posterior tuft neither beat continuously with metachronism nor display obvious undulating, "flagellum-like" movements. Rather, they adopt a rigid appearance most of the time (Fig. 1A–H), with just sporadic planar movements. We have seen sporadic sudden expansions of the entire tuft followed by rapid contractions. Such ciliary movements do not appear to be caused by external stimuli but are apparently induced internally by the larva. These rapid tuft movements usually cause brief accelerations of the larva, likely as a consequence of jet propulsion. Even if jet propulsion is thought to be an inefficient propulsion mechanism at low Reynolds numbers (Vogel 1994), it may help to enhance maneuverability. More importantly, our field observations of larvae of *I. oros* and *C. mollior* revealed that active use of the tuft by free-swimming larvae appears to be restricted to specific occasions. Unlike in the laboratory, most of the time larvae monitored in the field do not show active horizontal displacement by swimming. Rather, they

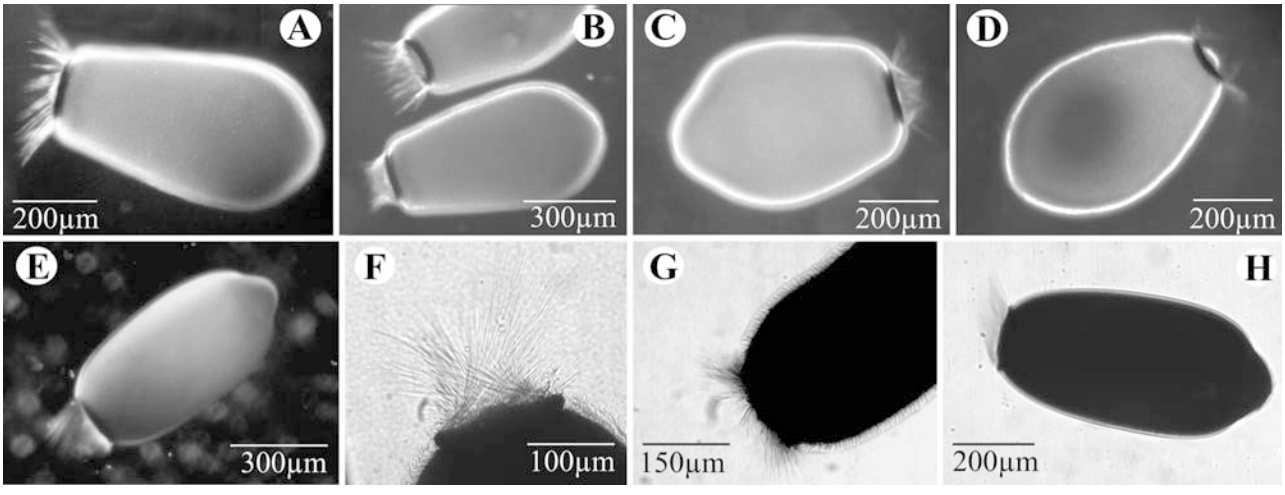

Fig. 1A–H General view of tufted parenchymellae belonging to *Sigmadocia caerulea* and *Ircinia oros*. Larvae of *S. caerulea* showing tufts in both expanded (**A**) and contracted (**B**) arrangement, respectively; note the posterior pigmented ring. **C**, **D** Larvae of *S. caerulea*, each showing half of its tuft expanded and the opposite half contracted. **E** Larva of *I. oros* showing a relaxed tuft. Note the posterior pigmented ring. Details of tufts in contracted (**F**) and expanded (**G**) tuft conformation, in *I. oros* larvae. **H** Larva of *I. oros* showing half of its tufts expanded and the opposite half contracted

maintain a vertical position, with the anterior pole oriented upward while rotating around their longitudinal axis. In this "resting attitude", larvae are passively dispersed by surge and currents that would overcome any larval attempt at directional swimming. We observed that active larval swimming in the field occurs only when drifting larvae encounter strong turbulence or enter the boundary layer of solid objects. Then, larvae regain the "horizontal position" (i.e., placing their longitudinal axis of the body parallel to the direction of movement with the anterior pole forward) by using the tuft and swimming actively. For unknown reasons, this latter swimming is that normally observed in most tufted parenchymellae when maintained in relatively small containers during laboratory experimentation.

Light-induced motion patterns

We have found that drastic changes in light intensity induce instantaneous movement of the cilia in the posterior tuft of all three species, but have no appreciable effects on the beating pattern of the anterior-lateral short cilia. Light-induced movement of the posterior cilia is clearly observable when larvae are placed on a slide and exposed to different levels of light intensity by opening and closing the shutter of a compound microscope. Under moderate levels of irradiance (100–180 μM photons m^{-2} s^{-1}), cilia of the tuft of all three species mostly lay parallel to the longitudinal axis of the larva (Figs. 1E, 2A). This ciliary arrangement, which makes the tuft look like a hollow cylinder, will be hereafter referred to as "relaxed". When light irradiance is increased above 200 ± 25 μM photons m^{-2} s^{-1}, the cilia of the tuft of both the photonegative *I. oros* and *C. mollior* (> 6-h-old) larvae suddenly move approximately 45° clockwise (as viewed from the anterior pole), slightly inclining themselves centripetally (Fig. 2B). This coordinated torsion-like movement of the cilia causes the tuft to close instantaneously in the form of a cone, the vertex of which points backward. This ciliary arrangement will be hereafter referred to as "contracted". When light intensity decreased below 50 ± 15 μM photons m^{-2} s^{-1}, posterior cilia move instantaneously counterclockwise (as viewed from the anterior pole), inclining themselves centrifugally. This movement causes the tuft to expand, adopting an "expanded arrangement" (Figs. 1A, G, 2C). Similar ciliary movements, but with an opposite sign, are seen in photopositive early (< 6-h-old) larvae of *C. mollior* and the photonegative larvae of *S. caerulea*. In these cases, the posterior tuft closes (Fig. 1F) under low irradiance and expands (Fig. 1G) under high irradiance. Each time irradiance is suddenly modified in a substantial way, the tuft of the larvae of all three species responds automatically, contracting and expanding instantaneously, as described above. This ability is maintained throughout the entire larval life, although the response of the cilia becomes increasingly slow when larvae enter the exploratory crawling phase prior to settlement. Furthermore, when larvae were bisected, and the posterior region placed under a light microscope, the tuft reacted to changes in irradiance as described above. This suggests that the ciliary movement in the tuft is not coordinated from the anterior part of the larva.

Laboratory observations of *I. oros* and late-stages of *C. mollior* larvae in the aquaria revealed that, when larvae swim from the shaded into the illuminated zone, they consistently (100% of larvae) deviate their

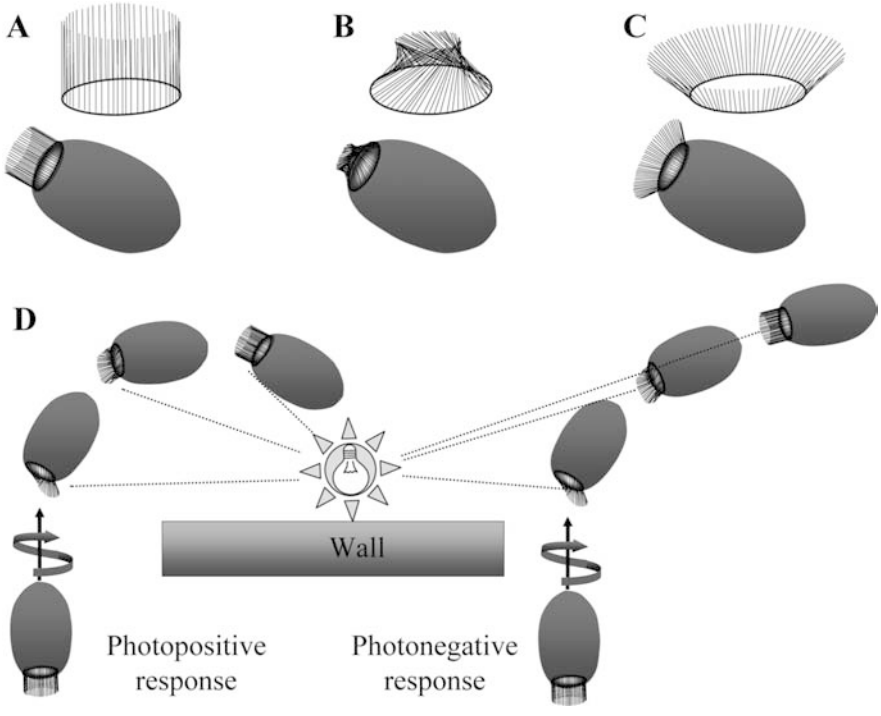

Fig. 2 Schematic drawing illustrating the larval tuft in relaxed (**A**), contracted (**B**), and expanded (**C**) conformation. **D** Diagram illustrating the swimming trajectory and changes in tuft conformation in photonegative and photopositive larval stages of *Cacospongia mollior* when entering an illuminated area from a shaded area

trajectory away from the light beam within a few seconds. While turning, the cilia on the illuminated side of the tuft adopt a contracted arrangement and the cilia on the shaded side of the tuft adopt an expanded arrangement (Figs. 1C, D, H, 2D). The irradiance-induced differential arrangement of the cilia on both sides of the tuft, coupled with larval clockwise rotation, likely causes the swimming trajectory to deviate toward the side in which the tuft is expanded, that is away from the light source (Fig. 2D). Deviation of the swimming trajectory persists until the plane of the posterior larval pole gets perpendicular to the direction of light. By this point, the larva is then swimming directly away from the light source, which means that all cilia in the tuft are receiving similar levels of irradiance. This causes the tuft to adopt a relaxed conformation and stop interfering with the trajectory generated by the metachronal beating of the short cilia that cover the body (Fig. 2D).

In the photopositive stage of *C.mollior* the response is inverted. The cilia on the illuminated side are expanded, which causes the larva to turn toward the light source (Fig. 2D). We did not make direct comparable observations of swimming trajectories of *S. caerulea,* but the ciliary photoresponse shown by these larvae under the compound microscope is similar to that described for the photopositive stage of *C. mollior*. However, such a ciliary arrangement would presumably make these photonegative larvae turn toward the light rather than swim away from the light source (see Discussion).

Cytological observations

Ciliated cells of anterior-lateral larval regions

These cells are by far the most abundant type in the larva. They virtually form the epithelium of the anterior and lateral regions, with only some unciliated cells (not shown) occasionally interspersed among the ciliated ones. The ciliated cells are typically columnar, 9–15 μm long and 1.5–3 μm wide, and have a marked distal–proximal polarity (Fig. 3A). The distal cell region bears a single cilium, usually emerging from a shallow, relatively symmetrical crypt (Fig. 3A–C). Nevertheless, some bi-ciliated cells, which are likely to be abnormal formations, may occur occasionally (Fig. 3D).

Cilia are about 15–20 μm long and 270–300 nm in diameter. Cross sections reveal that the axoneme consists of a "9×2 + 2" microtubule pattern, with the central pair of microtubule singlets circumferentially surrounded by nine microtubule doublets, and the whole structure surrounded by a typical bi-layer ciliary membrane (Figs. 3E, 4B, C). Each doublet is composed of one complete microtubule (subfibre A) and an incomplete microtubule (subfibre B), which shares three or four filaments from subfibre A. Internal and external dynein arms (with two and tree branches, respectively) originate from subfibre A and are directed toward subfibre B of the adjacent doublet (Figs. 3A, 4B, C).

Fig. 3A–L Cytology of the anterior-lateral ciliated epithelium. **A** Longitudinal section of an entire epithelial cell, showing a distal cilium and a proximal nucleus. **B** Longitudinal cell section showing the basal body, the basal foot connected to some microtubules, and the ciliary rootlet in close association with large mitochondria. **C** Longitudinal section of the basis of a cilium showing central microtubules that end above the plasmalemma, a stalked basal foot with two visible arms (distal and proximal) and two caps associated with microtubules, a fibrous, hollow ciliary rootlet, and diverse electron-clear vesicles. **D** Bi-ciliate cell in the lateral epithelium. **E** Cross section of a cilium view from the end to the base; note the typical 9×2 + 2 model and the dinein arms (*arrow*). **F** Cross section of a cilium at its base but above the transition region, showing the lumen folded by a two-layer membrane (*arrow*). **G** Cross section of a cilium at the level of the transition region showing a third, central singlet (*arrow*). **H** Cross section of a cilium immediately below the plasmalemma and just above the basal body, showing a circle of anchoring points. **I** Cross section of the proximal end of the basal body; note that the peripheral doublets become triplets connected to the surrounding anchoring points by the alar sheets. A basal foot is consistently located between doublets 6 and 8. **J**, **K** Two sequential longitudinal sections of the same cell showing details of a type I basal body and its associated basal foot, with enucleated cytoplasmic microtubules. **L** Cross section of several adjacent cells at the level of their basal body showing a consistent pattern in the orientation of the basal feet, which lay on the posterior side of the basal body

The proximal most axonemal portion, extending approximately 150–170 nm above the plasmalemma, shows a peculiar 9 + 3 model, in which a third singlet occurs (Figs. 3F, G, 4E). This additional singlet is consistently located along the line connecting the midpoint between the two main central singlets and that between the doublets 5 and 6. In this proximal region, the lumen of the axoneme is more electron-dense than the remaining axoneme (Fig. 3A–D); the lumen is folded by a two-layer membrane that surrounds the central singlets (Figs. 3F, G, 4D, E). The central singlets terminate at the proximal end of this basal axonemal region, just above the plasmalemma (Figs. 3B, C, 4A, E). In contrast, the peripheral doublets penetrate the cell cytoplasm (Figs. 3H, 4A), where they become a basal centriole (typically known as basal body or kinetosome) made of nine microtubule triplets (Figs. 3I, 4F). Because the central singlets of the axoneme do not pass the plasmalemma plane (Fig. 3C, D), the basal body is catalogued as type-II, according to Pitelka (1974).

The basal body is an electron-dense structure, measuring 170–190 nm in diameter and 300 nm in length. From the distal end of each triplet of the basal body, a radial, arc-shaped bundle of fibrils known as an alar sheet projects outward and slightly upward to contact an electron-dense sphere-like structure. This structure, called an anchoring point is also associated with the plasmalemma surrounding the cilium (Figs. 3H, I, L, 4A, F). Unlike typical cilia of many invertebrates, no particular cartwheel structure occurs in the lumen of the basal body at this level.

From the proximal end of the basal body emerges a fibrous, conical, and unbranched, ciliary rootlet (Figs. 3A–C, 4A). The rootlet shows no traces of

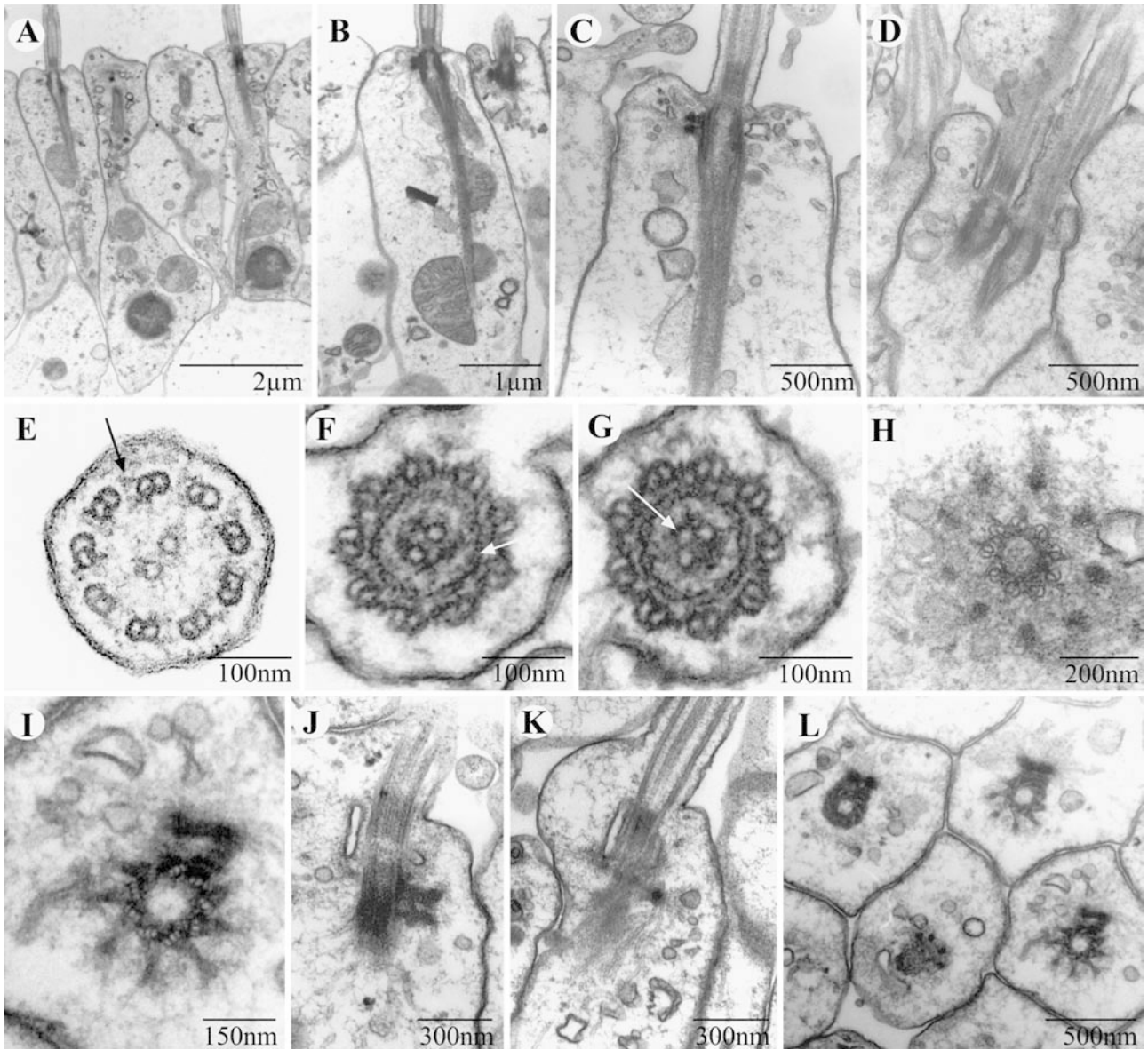

cross-striation and runs parallel to the longitudinal axis of the cell. It penetrates about 2.5–3.0 μm into the cytoplasm. The rootlet is closely flanked by large mitochondria, which may supply the energy required for ciliary beating (Fig. 3A, B).

There is a well developed basal foot besides the basal body (Fig. 3B, C), but no accessory centriole. The basal foot lies perpendicular to the basal body, and consistently emerges from triplets 6, 7 and 8. Therefore, it is located at the posterior side of the rootlet, coincidental with the direction of the effective stroke of the cilium (Figs. 3I, J, L, 4A). The structure of the basal foot is quite complex, but its fine substructure falls beyond the resolution of our TEM. In transverse sections, two parallel electron-dense rod-like structures, hereafter left and right arms, are seen to project from the posterior side of the basal body (Figs. 3I, L, 4G). Each arm ends in an electron-dense subspherical structure, hereafter basal foot cap, which is also connected transversally to its sister cap. The arms, which are less electron-dense than the caps, show some transversal bands. In the longitudinal cell sections, two arms, hereafter distal and proximal arms, are also visible and end in an electron-dense cap (Figs. 3J, 4A). Therefore, the basal foot consists of a total of four arms and four caps. Bundles of microtubules project from the caps of the basal body into the cytoplasm (Figs. 3B, C, K, 4A, G).

Apart from the structures described above, the cytoplasm of the distal region contains abundant electron-clear vesicles (Fig. 3A–D), which have been observed to fuse occasionally with the plasmalemma. The mid-cell region is mostly occupied by the ciliary rootlet, which is associated with large mitochondria. The proximal cell region contains a small Golgi apparatus, the nucleus, and a few, medium-sized vacuoles with lipidic and proteinic yolk. The nucleus, which never contacts the ciliary root, consistently lacks a nucleole, and shows a dense layer of peripheral chromatin

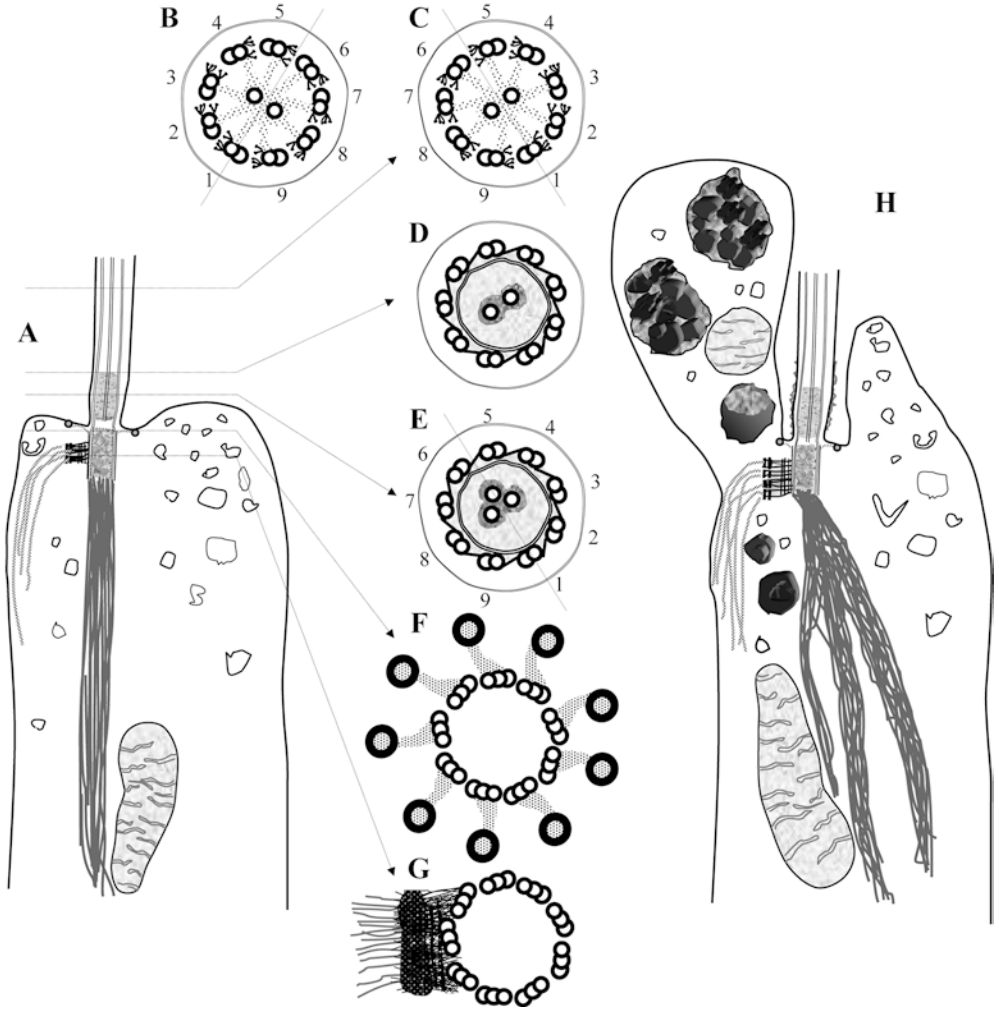

Fig. 4 **A** Schematic drawing showing the most relevant structures and organelles found in the longitudinal sections (A) and its corresponding cross-sections (**B–G**) in anterior-lateral ciliated cells. Axoneme sections viewed from the proximal to the distal end (**B**) and vice versa (**C**); note changes in doublet numbering and direction of dynein arms with change in section orientation. **D**, **E** Sections of the transition region at the proximal end of the axoneme illustrating the internal membrane that folds the lumen and a third central singlet at the proximal most level. Sections illustrating how the peripheral triplets of the basal body, which is type II, are connected to the "alar sheet"–"anchoring point" system (**F**) and the basal foot (**G**), respectively. **H** Longitudinal section of a cell in the posterior tuft showing a distal protrusion filled with pigment inclusions and mitochondria, a branched ciliary rootlet, a large basal foot, and type I basal body

(Fig. 3A). In the absence of specific TEM staining techniques for junction enhancing, we did not observe special membrane differentiations between adjacent ciliated cells. Likewise, we did not find any basement membrane or equivalent structure underlying the layer of ciliated cells.

Ciliated cells in the larval tuft

Posterior monociliated cells form a 10 to 20 cell-wide ring around the posterior larval pole, with their long cilia forming the tuft (Fig. 5A). The cytology of these cells is somewhat different from that of the ciliated cells in the lateral and anterior larval regions. They are columnar cells, being 1.5–4.0 μm wide. We failed to ascertain maximum cell length, but found that they were at least 10–12 μm long.

These cells are distinctive because they show one or more globate protrusions at the distal cell end that produces a markedly asymmetric crypt from which the cilium emerges (Figs. 4H, 5B, E). The position of the distal protrusion appears to change from cell to cell (Fig. 5B) and we suspect that protrusions of a group of contiguous cells are arranged in a fence-like structure that encircles a group of cilia (Fig. 6). Cross sections revealed cytoplasmic passageways connecting adjacent distal protrusions (Fig. 7A, B). These passageways consistently contained microtubules (Fig. 7B). We failed to obtain longitudinal sections of adjacent cells that showed these passageways, so it could not be established whether connections are between two distal protrusions of the same cell (intracellular passageways) or between protrusions of different cells (intercellular passageways). The first hypothesis is more likely, as syncytial organization has never been described in demosponges. Nevertheless, intercellular bridges could facilitate rapid cell-to-cell communication and coordination of tuft movements.

It is significant that these distal protrusions are filled with one or several mitochondria and electron-dense inclusions (Figs. 4H, 5B, 7A, 8A, B). The latter ones, irregular in shape and size, resemble pigment granules known from other invertebrates. They show a complex substructure, being membrane bounded and containing a set of non-homogeneous sub-granules and portions of membrane-like structures (Fig. 8D). These organelles are likely responsible for the pigmentation of the larval posterior ring (Fig. 1). Some scarce pigment granules

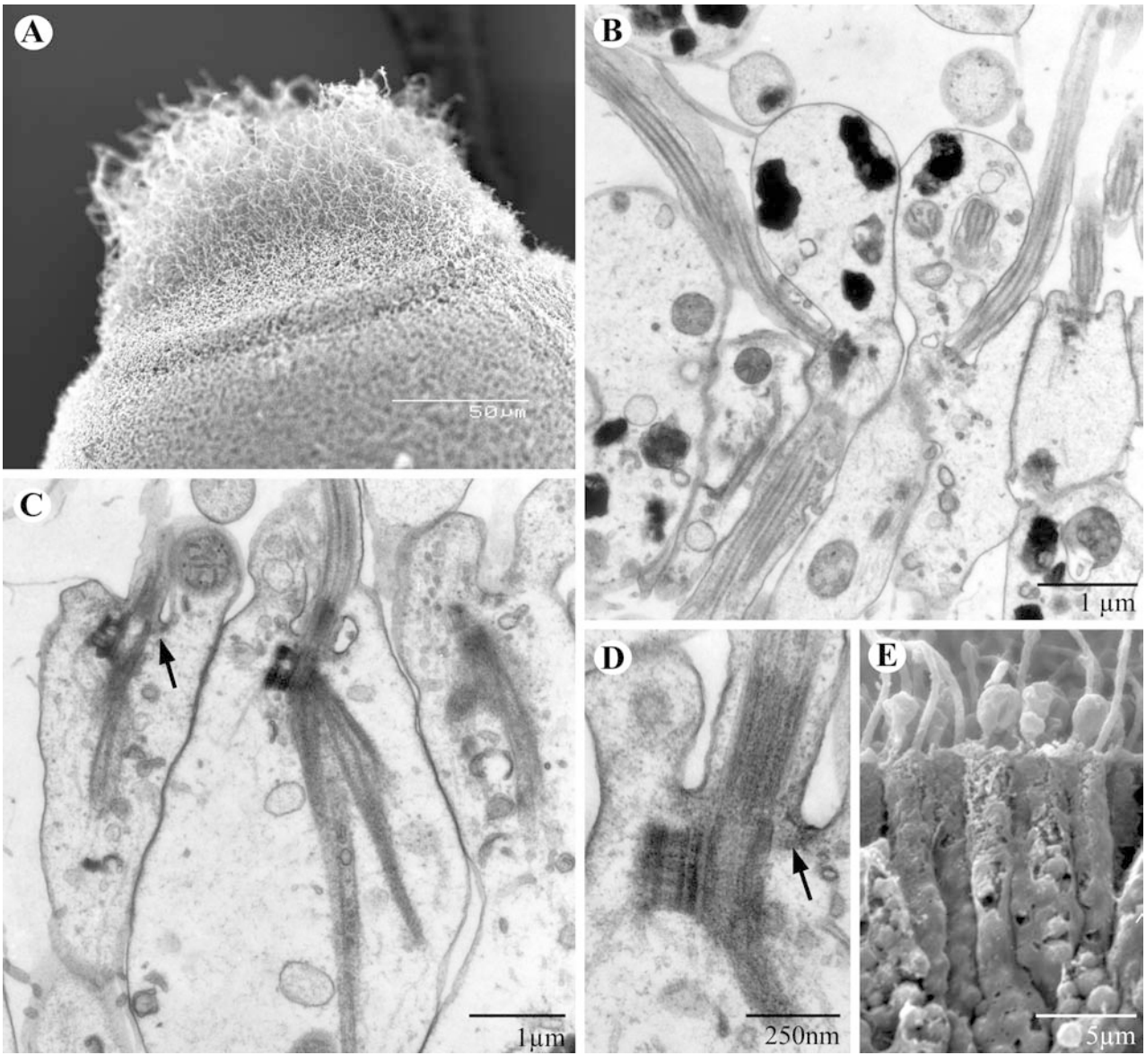

Fig. 5 **A** SEM micrograph of the posterior end of the *I. oros* larva. **B** Close-up of two ciliated cells of the tuft of an *S. caerulea* larva, showing the distal protrusions filled with pigment and mitochondria. **C** Close-up of branched ciliary rootlets and a type-I basal foot consistently located at the posterior side of the basal body; note the presence of a curved alar sheet and anchoring point (*arrow*). **D** Close-up of a basal body with central axonemal microtubule singlets ending at or even below the level of the surrounding plasmalemma, producing a type I basal body; note also the complex structure of the basal foot, with four visible arms and obvious transversal bands, and portions of alar sheets (*arrow*). **E** SEM micrograph of the ciliated cells in the tuft of an *I. oros* larva

also occur in the cytoplasm of the cells, usually close to the ciliary rootlets.

The axoneme of each cilium in the tuft is similar in structure to that in the ciliated cells of the remaining body, but longer. Electron microscopy observations corroborate the fact that the posterior long cilia are not substantially thicker than the remaining short cilia of the body (Figs. 3B, 5B). Surprisingly, unlike the short cilia of the body, the long cilia of the posterior tuft are visible to the naked eye (Fig. 1A–H). It appears that independent, microscopical axonemes of several contiguous monociliated cells lay in close contact. Further, they appear to function as a cohesive unit that is likely a peculiar type of compound cilia (Fig. 1). We suspect that such a supraciliary arrangement is facilitated by an encircling distribution of the distal protrusions of the cells (Fig. 6). No evidence of physical connections between adjacent cilia was found in the fixed larvae. However, unlike the case of the short cilia, a subtle glycocalyx occurs on the external side of the ciliary membrane in the proximal portion of these long cilia (not shown).

Longitudinal sections at the base of the cilia show that the central microtubules appear to end either just at or immediately below the level of the plasmalemma. This means that the basal body, unlike that of the short-cilium cells, is type-I (Fig. 5D). The existence of three central singlets in these cells could not be confirmed

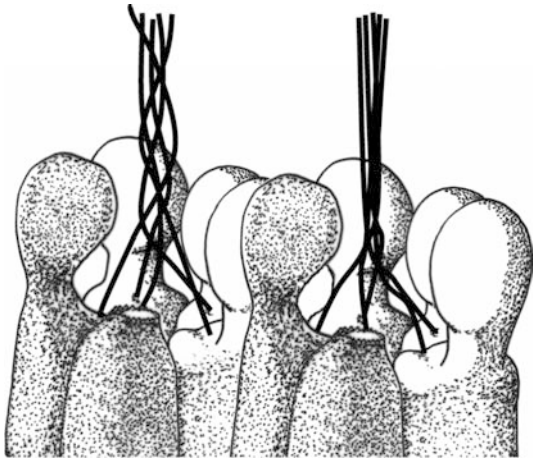

Fig. 6 Diagram of the suggested arrangement of cilia and distal cell protrusions to form functional beating units

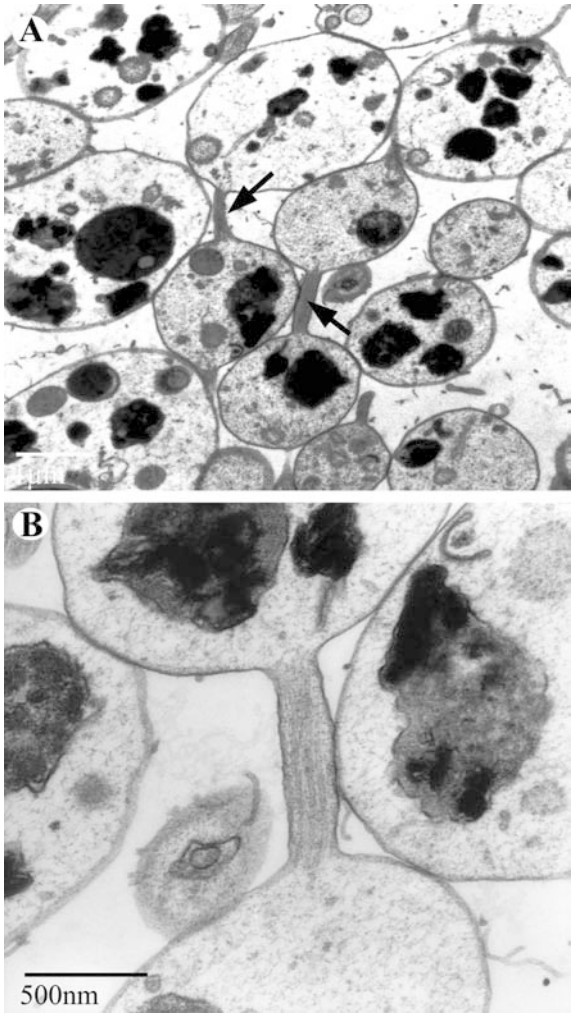

Fig. 7A, B Transverse sections of distal protrusions of cells in the tuft. **A** Adjacent protrusions, filled with mitochondria and pigment inclusions, and connected by cytoplasmic bridges containing microtubules (*arrows*). **B** Detail of microtubules within an inter-protrusion cytoplasmic bridge; note the irregular structure of pigment inclusions, which are membrane-bound

Fig. 8 A General view of the transition region between the lateral epithelium and the tuft, the latter characterized by the presence protrusions filled with pigment. **B** General view of the transition region between the tuft and the unciliated posterior epithelium, the latter characterized by large globate cells charged with very large vacuoles (*arrow*). **C** General view of the posterior unciliated epithelium. **D** Comparative view showing the irregular structure of pigment granules occurring in the distal protrusions of the tuft cells (to the *left*) versus the homogeneous aspect of the inclusions in the posterior unciliated cells. **E** Detail of a posterior unciliated cell showing the large electron-dense vacuoles and an eccentric anucleolated nucleus (*arrow*). **F** Detail of vacuole in the unciliated posterior cell showing a multiplayer membrane-like structure

because we could not obtain transverse sections that revealed this trait. The occurrence of alar sheets and anchoring points was evident in several sections (Fig. 5C, D).

It is also significant that the basal body and the ciliary rootlets are far more developed in the cells of the tuft than in the remaining ciliated cells. The basal body shows an arrangement and basic structure similar to that described for the cells with short cilia, yet is larger in length (Figs. 4H, 5C, D). Longitudinal sections reveal four caps and four arms, instead of just two of each. Transversal sections show just two arms and two caps, as in basal feet of the anterior-lateral ciliated cells. Therefore, the basal foot of these cells consists of a total of eight arms and eight caps. The ciliary rootlet is similar to that of the short cilia in that it is fibrous and hollow, and lacks cross-striation. Nevertheless, it is branched and develops several subfibers that do not run parallel to the longitudinal axis of the cell but deviate toward the anterior region, opposite to the side in which the basal body lies (Figs. 4H, 5C).

Like in the ciliated cells of the body, the mid-region of the cells in the tuft is occupied by the ciliary rootlets, associated mitochondria, and some scattered pigment granules. The proximal region contains some pigment granules, some mitochondria, the Golgi apparatus (not shown), and an anucleolate nucleus characterized by an irregular layer of peripheral chromatin. No observations were made of the special membrane junctions between adjacent ciliated cells in the tuft nor between the basal region of these tuft cells and the underlying cells.

Unciliated cells of the posterior pole

The hindmost surface of the larva, which is encircled by the tuft, consists of a pseudoestratified layer of subglobate unciliated cells (Fig. 8B, C). They are 5–7 μm in diameter, have an eccentric, anucleolate nucleus, and several large, electron-dense vacuoles (Fig. 8C–F). Vacuoles are surrounded by a multilayered membrane and contain relatively homogenous but finely granulose material of an uncertain nature (Fig. 8D–F). The structure of the vacuole contents is neither crystalline nor paracrystalline, which is typically observed in

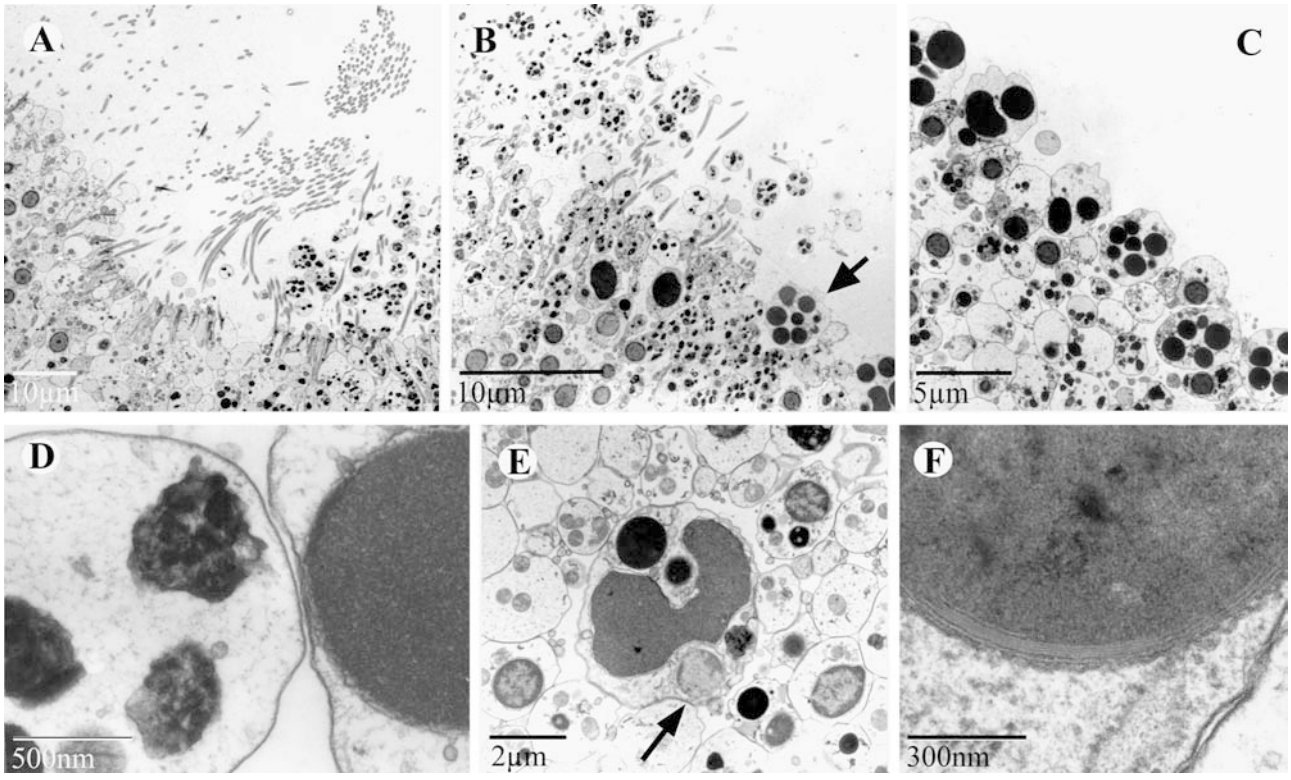

proteins. It is also not completely homogeneous, which is typically the case with lipidic inclusions seen in some internal cells of these larvae.

Discussion

Larval photobehavior

Our results partially support the idea of Leys and Degnan (2001), in that the individual ciliary photoresponses of each cell in the posterior tuft are responsible for the directional deviation of the larval trajectory with respect to light. The ability to detect the presence of light and produce an automatic light-induced ciliary movement allows sponge larvae to make directional swimming responses to light cues, even when their unspecialized photoreceptors cannot provide any discrimination of light direction. It appears that in the absence of both gap junctions and neuronal networks for rapid intercellular communication, the individual responses of tuft cells become externally coordinated by their respective levels of cyclic exposure to light on the rotating, forward-moving larvae. Nevertheless, the hypothesis that cytoplasmic bridges interconnecting the distal protrusion of adjacent cells are involved in coordination of tuft movements cannot be ruled out. The shading effect of the pigment-filled protrusions in the tuft cells apparently helps to emphasize differences in light exposure between cell groups. This is a common feature in very simple eyecup photoreceptors of many lower invertebrates which cannot form any image, yet are able to discriminate the direction of light by localizing the position of the shadow projected by shading structures on a photoexcitable surface (Cronin 1986). By analogy, the posterior larval ring of pigmented photosensitive cells, which are extraocular photoreceptors, may work similarly to a larval eyecup.

In the larvae studied, the posterior cilia appear to have a dual role; they serve as both receptors and effectors of the photoresponse. This was previously suggested from behavioral evidence (Maldonado and Young 1996). Interestingly, the long cilia of several adjacent cells can apparently join in groups. Each group then appears to beat as a cohesive unit. The existence of these supraciliary groups has also been inadvertently described in an illustration of the tufted parenchyemella of the haplosclerid *Reniera* sp. (Leys and Degnan 2001; see their Fig. 8B, C), although the authors did not recognize such a ciliary pattern. To our knowledge, compound cilia made by monociliated cells are known to exist in the anthozoan larva *Zoanthina* sp. and phoronid larvae (Nielsen 1987). Cilia in the apical tuft of the cnidarian planula of *Anthopleura* sp. also beat as a unit, although no physical connection between its monociliated cells has been found (Chia and Koss 1979).

In photonegative larvae of *I. oros* and *C. mollior*, which expand their tuft under low levels of irradiance, it is easy to explain how larvae passively deviate from a light source. Their tuft arrangement, contracted on the illuminated side of the larval body and expanded on the shaded side, is sufficient to passively deviate the larval trajectory away from the light source. However,

it remains unclear how such a deviation is achieved by the photonegative larva of *S. caerulea* and that of *Reniera* sp. (Leys and Degnan 2001). No accurate observations on the conformation of the tuft when free-swimming larvae of these species enter an illuminated area from a shaded area have been made. However, these larvae expand the whole tuft when exposed to high irradiance under a compound microscope, and pictures (Fig. 1C, D) indicate that the illuminated side of the tuft is usually expanded while the shaded side is contracted. Such a tuft arrangement should make these larvae turn toward light rather than move away. It has been proposed by Leys and Degnan (2001) that the cilia on the illuminated side, apart from expanding, would beat more rapidly, which would cause the larva to turn away from light. Such a suggestion needs further investigation, since photonegative larvae of the order Haplosclerida (i.e., *Reniera* and *Sigmadocia*) and those of the order Dictyoceratida (i.e., *Ircinia* and *Cacospongia*) would be expected to have developed similar response mechanisms.

The presence of a ciliary tuft in parenchymellae, regardless of the tuft's photoreceptor function, appears to increase larval ability to accelerate and maneuver (Konstantinova 1966; Woollacott 1993; Maldonado and Young 1996). This has also been suggested for other invertebrate larvae (Chia et al. 1983). Hence, from the point of view of motion, tufted parenchymellae probably can exploit boundary layers and settle suitable microhabitats better than non-tufted sponge larvae. Details of how effective these hypothetical differences are in the field remain uninvestigated. Interestingly, our field observations of *I. oros* and *C. mollior* indicate that larvae drift most of the time in the water column, and do not exploit the enhanced power and maneuverability provided by the tuft. Drifting behavior has also been observed (authors unpublished) in the field with a variety of tufted (*Ircinia variabilis* and *Haliclona* sp.) and non-tufted parenchymellae (*Crambe crambe* and *Mycale* sp.) species. Previous laboratory studies on a non-tufted larva (*Scopalina lophyropoda*; Uriz et al. 1998) and tufted larvae (Leys and Degnan 2001) report that larvae can adopt a vertical position several hours after being in the aquaria. Therefore, it appears that light-induced tuft movements in the field are mostly useful toward the end of the free-swimming period, when larvae explore the substrata for suitable settlement sites.

In contrast to the consistent tuft behavior shown by the larvae in this study and those in Leys and Degnan's (2001) research, there may be tufted parenchymellae in which the posterior cilia do not straighten, and are not constrained to beat in a plane (planar beating). Unpublished observations of the larva of *Halichondria magniconulosa* (see Maldonado and Young 1996) revealed that cilia in the tuft display a flagellum-like movement most of the time. Therefore, we cannot discard the possibility that tufted larvae of halichondrid sponges effect their photoresponse by an alternative mechanism to what we and Leys and Degnan (2001) report for tufted larvae of sponges belonging to the orders Haplosclerida, Dendroceratida and Dictyoceratida.

The photoreceptory mechanism

In most invertebrate and vertebrates, the cells specialized in photoreception have disks or microvilli that extensively increase the membrane surface upon which a photopigment is generally exposed. In some little-sophisticated cilium-derived photoreceptors of invertebrates (e.g., cnidarians, echinoderms, etc), the expansion of the membranes only affects the proximal portion of the ciliary membrane and the distal region of the plasmalemma surrounding the cilium (Eakin 1963). In this context, the distal protrusions in the putative photosensory cells of the parenchymella can be interpreted as a rudimentary mechanism to increase cell-membrane surface. A common feature of both vertebrate and invertebrate photoreceptors is that mitochondria are situated near the light-sensitive apparatus. This suggests that intense oxidative metabolism is associated with photoreception (Eakin 1963). The presence of mitochondria in the distal protrusions of the tuft cells is noteworthy, as they are not present in the distal positions in any other epithelial cell of the parenchymella. We believe that this fact strongly supports the photosensitivity of these cells. It is also documented that the central pair of microtubules disappears toward the distal portion of the axoneme in the photoreceptive cilia of many invertebrates (e.g., Blumer et al. 1995; Blumer 1998). Regrettably, we failed to ascertain whether this is also the pattern in the cilia of the larval tuft. The fact that the cilium of the putative photosensitive cells is mobile appears to conflict with a potential photosensitive role. Most metazoan photoreceptors that are based on ciliated cells are characterized by the presence of modified, immobile cilia (Eakin and Hermans 1988). However, it can be argued that the low level of cell differentiation inherent in the primitive status of the Porifera may have forced the photoreceptor cells to also act as effector cells. In this regard, the occurrence of light-induced ciliary movements in the tuft of bisected larvae suggests that there is little or no involvement of the cells on the lateral and anterior areas of the larval epithelium in the photoresponse. Photoresponse models in which the sensitive cells are also the effectors occur in unicellular and colonial protozoans rather than in metazoans (Wolken 1995). Further evidence of the primitive nature of the photoresponse system is that the shading pigment is not provided by accessory cells and occurs within the putative photoreceptor cells. Again, this is a mechanism typical of photoreceptors in protozoans and lower invertebrates such as cnidarians (Singla 1974; Weiss et al. 1985; Thomas et al. 1987; Blumer et al. 1995).

At the molecular level the photoreceptor remains unidentified. In the absence of any obvious ultrastructural

connection between pigmentary and ciliary organelles, it is likely that the photoreception system is based on a photo-excitable molecule associated with either the ciliary membrane or the basal apparatus (basal body + basal foot). Unfortunately, the ability to confirm this falls beyond the resolution of conventional TEM. Additional studies are needed to determine how light characteristics (e.g., intensity, spectral composition, polarization) elicit larval responses. Such studies should incorporate cytochemical approaches, which can achieve a finer localization of putative light-excitable compounds.

A single attempt to investigate the spectral sensitivity of photoresponsive sponge larvae has been made to date (Leys et al. 2002). The results indicate that the tufted parenchymellas of the haplosclerid *Reniera* sp. respond most to blue (440 nm) and orange–red light (600 nm). Such observations apparently suggest that the photoreceptive pigment may be a flavin or carotenoid. However, further investigations are needed to corroborate such a conclusion, since a combination of pigments or short-wavelength-absorbing rhodopsins could also be responsible for the action spectrum detected. Indeed, rhodopsins, rather than flavins or carotenoids, act as a photosensitive pigment not only in most multicellular animals, but also green algae (Foster et al. 1984) and fungus zoospores (Saranak and Foster 1997). It is well established in flagellate green algae that membrane-associated rhodopsin molecules undergo conformational changes when excited by light and cause the opening of ion channels and inward Ca^{++} flux (Harz and Hegemann 1991; Hegemman 1997). Intra-cellular levels of Ca^{2+} can regulate ciliary beating, as has been demonstrated in permeabilized cells (Kamiya and Witman 1984). This may also be the basic system underlying the sponge photoresponse, but future work combining action spectroscopy with microspectrophotometry would be needed to clarify this issue, as also suggested by Leys et al. (2002).

The potential role of the posterior unciliated cells in the photoresponse remains unclear. These cells, though consistently charged with large electron-dense vacuoles, appear to vary in morphology across species. In the non-tufted parenchymella of the poecilosclerid *Hamigera hamigera*, the unciliated surface of the posterior pole is made up of a layer of subtriangular or subcylindrical cells, the cytoplasm of which is rich in filamentous–granulose inclusions (Boury-Esnault 1976). In the tufted parenchymella of *Haliclona tubifera*, the posterior unciliated surface is smooth and made of cells that are flattened, irregular in shape, and rich in 1-μm electron-dense granules (Woollacott 1993). Amano and Hori (1994) found that the cells of the unciliated posterior surface of the tufted parenchymella of the haplosclerid *Haliclona permollis* were archeocytes similar to those occurring in the innermost region of the larva. In contrast, globose-pseudocolumnar cells containing large electron-dense mucus-like inclusions form the posterior unciliated surface of the tufted parenchymella of *Reniera* sp. (Leys and Degnan 2001). We found cells with a morphology and arrangement similar to that described by Leys and Degnan (2001). The actual composition of the inclusions in these posterior cells remain speculative, since cytochemical evidence is lacking in virtually all cases. Because posterior cells are usually charged with large electron-dense vacuoles, it is conceivable that they may serve as a multicellular lens-like structure. Such a structure may be necessary both to laterally shield the photoreceptor cells of the tuft and to provide a cut-off filter for short wavelengths that otherwise would damage exposed unciliated posterior cells and underlying tissue.

Remarkable cytological features

Several cytological features are important to consider, irrespective of their implication for larval photoreception, because they may have significance in understanding parenchymella cytology within the context of the lower invertebrates.

The structure of the proximal portion of the axoneme of the larval cilia, showing three central singlets, is remarkable. This "9×2 + 3" model is only known from the immobile, photoreceptory cilia of the ocelli of the scyphozoan polyp of *Stylocoronella* (Cnidaria). The situation is even atypical for Scyphozoa, and Cnidaria, as ocelli are typically restricted to the medusa stage (Blumer et al. 1995). The functional significance of this accessory singlet remains unknown.

It is also noteworthy that the central singlets of axonemal microtubules of the short cilia terminate above the level of the surrounding plasmalemma (type II basal body, according to Pitelka 1974). In contrast, the central singlets of the cilia in the tuft terminate at the level of the surrounding membrane (type I basal body). In Porifera, this latter model has only been documented in the choanocytes of the freshwater sponge *Ephydatia fluviatilis* (Brill 1973; Woollacott and Pinto 1995). Type I basal bodies are characteristic of ciliate protozoans, birds and mammals (Pitelka 1974; Sanderson 1984). Type II basal bodies are predominant in lower vertebrates, invertebrates (sponges included), some fungi, and many flagellate protozoans (Pitelka 1974; Woollacott and Pinto 1995). The functional significance of the difference in the basal body between the anterior-lateral and tuft cells of the parenchymella remains unclear.

We also found that the lumen of the basal body in the larval cilia is atypical. In most animal cilia, the lumen is occupied at its proximal end by nine radiating electron-dense fibrils, each connecting the center of the lumen with the inner most subfibre (A) of the triplets. Such an arrangement causes the characteristic cartwheel structure reported from basal body cross-sections (Sanderson 1984). Instead, we found a two-layered membrane folding the lumen of the basal body, a structure described in Porifera for the first time. We also found that the basal body is connected to the surrounding plasmalemma by

alar sheets and anchoring points. These structures have only been described previously in sponge larvae by Woollacott and Pinto (1995). Our findings support their suggestion that alar sheets and anchoring points are common features in cilia of sponge larvae. So far, such structures have never been reported from ciliated cells (choanocytes, endopinacocytes) of adult sponges. Nevertheless, they are common in cilia of other invertebrates and vertebrates. They appear to be responsible for reinforcing the anchorage of the basal body and palliating the traction exerted during the ciliary beating.

There are several structures associated with the basal body of many invertebrates, such as a basal plate, an accessory centriole, and lateral arms, which do not occur in the larvae we studied. However, accessory centrioles and diverse lateral arms occur in larvae of several other sponge species (Woollacott and Pinto 1995), producing a presence/absence pattern that appears to have no phylogenetic significance.

A relevant structure associated with the basal body is the basal foot, which is widespread in metazoans and rare in protists (see review by Woollacott and Pinto 1995). The structure of the basal foot in the studied parenchymellae is similar to that of the "stalked basal foot" described by Woollacott and Pinto (1995). Our findings are consistent with several previous reports on basal feet in sponge larvae, which support the view that stalked basal feet typically occur in both haplosclerid (Woollacott 1993; Amano and Hori 1996; Leys and Degnan 2001) and keratose sponges (Woollacott and Pinto 1995). Interestingly, we have found the basal foot of tuft cells to be approximately twice the size of that of cells from the anterior-lateral regions. Leys and Degnan (2001) apparently did not report these differences in their study on *Reniera*, but their SEM figures strongly suggest that basal feet of more than one size occur in these larvae. From our approach, it remains unclear whether size differences are related to the need to physically support the beating of longer cilia, or to a role in the photoresponse. It is noteworthy that basal feet are always positioned on the posterior side of the basal body, just in the direction of the effective stroke of the larval cilia. This arrangement suggests that the above-mentioned differences may be related to the need to support a more powerful stroke by the longer cilia in the tuft. Nevertheless, the basal foot also appears to be a center for microtubule nucleation, a role usually played by the centrosome in other animal cells. In some invertebrates, basal feet appear to have a relevant role in determining the spatial distribution of cilia of multiciliated cells, and are also essential for coordination of beating (Gordon 1982; Hard and Rieder 1983; Sandoz et al. 1988). We have occasionally found bi-ciliated cells in the lateral larval epithelium (Fig. 3D), although we have failed to ascertain whether each cilium possessed its own basal foot. Bi-ciliated cells have also been described in the non-tufted parenchymella of the poecilosclerid sponge *Mycale contarenii* by Lévi (1964), who regarded them as the result of a defective cell division.

Finally, we found a ciliary rootlet in association with the proximal end of the basal body. It is unbranched in anterior-lateral epithelial cells, but branched in tuft cells. Again, we cannot ascertain whether this difference is related to the need to support the motion of a longer cilium in the tuft cells or the putative photoreceptor role of these cells. In both cell types, the rootlet is fibrous and lacks the typical cross-striation that characterizes ciliary rootlets in the remaining metazoans. At present, the presence of cross-striated rootlets in Porifera has only been demonstrated convincingly for the four studied larvae of the class Calcarea. There is also a report by Lévi (1964) that mentions the presence of a cross-striated rootlet in larval cilia of the demosponge *Mycale contarenii*. However, the validity of such a report should be reconsidered, since a recent study by Woollacott and Pinto (1995) on the larva of the congeneric *Mycale cecilia* found only non-striated rootlets. Within the Porifera, there are also further differences in the structure of the rootlet, which in some larvae is organized as fibrous bundles and in others as a set of parallel lamellae (reviewed by Woollacott and Pinto 1995). So far, there is not enough available information to ascertain the significance of such structural diversity.

This study agrees with other recent studies in that the cytology of sponge larvae is relatively complex and that the functionality of diverse singular structures remains unclear. It appears that further cytological investigations involving different larval types and using a combination of cytochemical, physiological and ecological approaches are needed to elucidate not only the fine mechanisms of photoresponse, but also the functional significance of diverse anatomical singularities in these larvae.

Acknowledgements This study was supported by the Fulbright Association (FU-93-02207057) and two research grants from the Spanish government to M.M. (MEC-PB-98-0485; BMC-2002-01228). This is HBOI contribution number 1515 and SMSFP contribution number 563.

References

Amano S, Hori I (1994) Metamorphosis of a demosponge. I. Cell and structure of swimming larva. Invertebr Reprod Dev 25:193–204

Amano S, Hori I (1996) Transdifferentiation of larval flagellated cells to choanocytes in the metamorphosis of the demosponge *Haliclona permollis*. Biol Bull 190:161–172

Bergquist PR, Sinclair ME (1968) The morphology and behavior of larvae of some intertidal sponges. N Z J Mar Freshw Res 2:426–437

Bergquist PR, Sinclair ME, Green CR, Silyn-Roberts H (1979) Comparative morphology and behaviour of larvae of Demospongiae. In: Lévi C, Boury-Esnault N (eds) Biologie des spongiaires. CNRS, Paris

Blumer MJ (1998) Alterations of the eyes of *Carinaria lamarcki* (Gastropoda, Heteropoda) during the long pelagic cycle. Zoomorph 118:183–194

Blumer MJF, Salvini-Plawen L, Kikinger R, Büchinger T (1995) Ocelli in a Cnidaria polyp: the ultrastructure of the pigment spot in *Stylocoronella riedli* (Scyphozoa, Stauromedusae). Zoomorph 115:221–227

Bourget E, DeGuise J, Daigle G (1994) Scales of substratum heterogeneity, structural complexity, and early establishment of a marine epibenthic community. J Exp Mar Biol Ecol 181:31–51
Boury-Esnault N (1976) Ultrastructure de la larve parenchymella d'*Hamigera hamigera* (Schmidt) (Démosponge, Poecilosclerida). Origine des cellules grises. Cah Biol Mar 17:9–20
Brill B (1973) Untersuchungen zur ultrastruktur der choanocyte von *Ephydatia fluviatilis* L. Z Zellforsch Mikrosk Anat 144:231–245
Chia F-S, Koss R (1979) Fine structural studies of the nervous system and the apical organ in the planula larva of the sea anemone *Anthopleura elegantissima*. J Morphol 160:275–298
Chia F-S, Buckland-Nicks J, Young CM (1983) Locomotion of marine invertebrate larvae: a review. Can J Zool 62:1205–1222
Cronin TW (1986) Photoreception in marine invertebrates. Am Zool 26:403–415
Eakin RM (1963) Lines of evolution of photoreceptors. In: Mazia D, Tyler A (eds) General physiology of cell specialization. McGraw-Hill, New York
Eakin RM, Hermans CO (1988) Eyes. Microf Mar 4:135–156
Evans CW (1977) The ultrastructure of larvae from the marine sponge *Halichondria moorei* Bergquist (Porifera, Demospongiae). Cah Biol Mar 18:427–433
Fell PE (1974) Porifera. In: Giese AC, Pearse JS (eds) Acoelomate and pseudocoelomate metazoans. Academic Press, New York and London
Forward RB, Cronin TW, Stearns DE (1984) Control of diel vertical migration: photoresponses of a larval crustacean. Limnol Oceanogr 29:146–154
Foster KW, Saranak J, Patel N, Zarilli G, Okabe M, Kline T, Nakanishi K (1984) A rhodopsin is the functional photoreceptor for phototaxis in the unicellular eucaryote *Chlamydomonas*. Nature 311:756–759
Fry WG (1971) The biology of larvae of *Ophlitaspongia seriata* from two North Wales populations. Fourth European Mar Biol Symp:155–178
Gordon RE (1982) Three-dimensional organization of microtubules and microfilaments of the basal apparatus of ciliated respiratory epithelium. Cell Motil 4:385–391
Hard R, Rieder CL (1983) Muciliary transport in newt lungs: the ultrastructure of the ciliary apparatus in isolated epithelial sheets and in functional triton-extracted models. Tissue Cell 15:227–243
Harz H, Hegemann P (1991) Rhodopsin-regulated calcium currents in *Chlamydomonas*. Nature 351:489–491
Hegemann P (1997) Vision in microalgae. Planta 203:265–274
Hills JM, Thomason JC, Milligan JL, Richardson M (1998) Do barnacle larvae respond to multiple settlement cues over a range of spatial scales? Hydrobiologia 375/376:101–111
Jaeckle WB (1995) Transport and metabolism of alanine and palmitic acid by field-collected larvae of *Tedania ignis* (Porifera, Demospongiae): estimated consequences of limited label translocation. Biol Bull 189:159–167
Kamiya R, Witman GB (1984) Submicromolar levels of calcium control the balance of beating between the two flagella in demembranated models of *Chlamydomonas*. J Cell Biol 98:97–107
Kaye HR, Reiswig HM (1991) Sexual reproduction in four Caribbean commercial sponges. III. Larval behaviour, settlement and metamorphosis. Invertebr Reprod Dev 19:25–35
Konstantinova MI (1966) Characteristic of movement of pelagic larvae of marine invertebrates. Dokl Akad Nauk SSSR 170:726–729
Lévi C (1964) Ultrastructure de la larve parenchymella de Démosponge. I. *Mycale contarenii* (Martens). Cah Biol Mar 5:97–104
Leys SP, Degnan BM (2001) Cytological basis of photoresponsive behavior in a sponge larva. Biol Bull 201:323–338
Leys SP, Cronin TW, Degnan BM, Marshall JN (2002) Spectral sensitivity in a sponge larva. J Comp Physiol [A] 188:199–202
Maldonado M, Bergquist PR (2002) Phylum Porifera. In: Young CM, Sewell MA, Rice ME (eds) Atlas of marine invertebrate larvae. Academic Press, San Diego
Maldonado M, Uriz MJ (1998) Microrefuge exploitation by subtidal encrusting sponges: patterns of settlement and post-settlement survival. Mar Ecol Prog Ser 174:141–150
Maldonado M, Young CM (1996) Effects of physical factors on larval behavior, settlement and recruitment of four tropical demosponges. Mar Ecol Prog Ser 138:169–180
Maldonado M, Young CM (1999) Effects of the duration of the larval life on post-larval stages of the demosponge *Sigmadocia caerulea*. J Exp Mar Biol Ecol 232:9–21
Maldonado M, George SB, Young CM, Vaquerizo I (1997) Depth regulation in parenchymella larvae of a demosponge: relative roles of skeletogenesis, biochemical changes and behavior. Mar Ecol Prog Ser 148:115–124
Nielsen C (1987) Structure and function of metazoan ciliary bands and their phylogenetic significance. Acta Zool (Stockholm) 68:205–262
Pitelka DR (1974) Basal bodies and root structures. In: Sleigh MA (ed) Cilia and flagella. Academic Press, New York
Raimondi PT (1990) Patterns, mechanisms, consequences of variability in settlement and recruitment of an intertidal barnacle. Ecol Monogr 60:283–309
Sanderson MJ (1984) Cilia. In: Bereiter-Hahn J, Matoltsy AG, Richards KS (eds) Biology of the integument. 1. Invertebrates. Springer, Berlin Heidelberg New York
Sandoz D, Chailley B, Boisvieux-Ulrich E, Lemullois M, Laine M-C, Bautista-Harris G (1988) Organization and functions of cytoskeleton in metazoan ciliated cells. Biol Cell 63:183–194
Sarà M, Vacelet J (1973) Ecologie des Démosponges. In: Grassé PP (ed) Spongiaires. Anatomie, physiologie, systématique, ecologie. Masson, Paris
Saranak J, Foster KW (1997) Rhodopsin guides fungal phototaxis. Nature 387:465–466
Singla CL (1974) Ocelli of Hydromedusae. Cell Tissue Res 149:413–429
Thomas MB, Freeman G, Martin VJ (1987) The embryonic origin of neurosensory cells and the role of nerve cells in metamorphosis in *Phialidium gregarium* (Cnidaria, Hydrozoa). Invert Biol 11:265–287
Uriz MJ, Maldonado M, Turon X, Martí R (1998) How do reproductive output, larval behaviour, and recruitment contribute to adult spatial patterns in Mediterranean encrusting sponges? Mar Ecol Prog Ser 167:137–148
Uriz MJ, Turon X, Becerro MA (2001) Morphology and ultrastructure of the swimming larvae of *Crambe crambe* (Demospongiae, Poecilosclerida). Invertebr Biol 120(4):295–307
Vacelet J (1979) Quelques stades de la reproduction sexuel d'une éponge Sphinctozoaire actuelle. In: Lévi C, Boury-Esnault N (eds) Biologie des spongiaires. CNRS, Paris
Vogel S (1994) Life in moving fluids. The physical biology of flow. Princeton University Press, Princeton, N.J.
Walters LJ, Wethey DS (1996) Settlement and early post-settlement survival of sessile marine invertebrates on topographically complex surfaces: the importance of refuge dimensions and adult morphology. Mar Ecol Prog Ser 137:161–171
Weis VM, Keene DR, Buss LW (1985) Biology of hydractiniid hydroids. 4. Ultrastructure of the planula of *Hydractinia echinata*. Biol Bull 168:403–418
Wolken JJ (1995) Light detectors, photoreceptors, and imaging systems in nature. Oxford University Press, New York
Woollacott R (1990) Structure and swimming behavior of the larva of *Halichondria melanodocia* (Porifera: Demospongiae). J Morphol 205:135–145
Woollacott RM (1993) Structure and swimming behavior of the larva of *Haliclona tubifera* (Porifera: Demospongiae). J Morphol 218:301–321
Woollacott RM, Pinto RL (1995) Flagellar basal apparatus and its utility in phylogenetic analyses of the Porifera. J Morphol 226:247–265
Young CM, Chia F-S (1984) Microhabitat-associated variability in survival and growth of subtidal littoral ascidians during the first 21 d after settlement. Mar Biol 81:61–68